Supporting Information

Solvation Configuration and Interfacial Chemistry Regulation via Bio-based Cyrene Additive for Highly Reversible Zinc Anode

*Chang Li,[1,2] Yang Song,[1,2] Ning Gao,[1] Can Ye,[1] Xuebing Xu,[1,2] Weisheng Yang,[3] and Chaoquan Hu[1,2,]**

1. Nanjing IPE Institute of Green Manufacturing Industry, Nanjing, Jiangsu, 211135, P. R. China
2. State Key Laboratory of Mesoscience and Engineering, Institute of Process Engineering, Chinese Academy of Sciences, Beijing, 100190, P. R. China
3. College of Materials Science and Engineering, Nanjing Forestry University, Nanjing, Jiangsu, 210037, P. R. China

*Corresponding author:
Tel. & Fax: +86-25-86107053
E-mail: cqhu@ipe.ac.cn (C. Hu)

Contents

Experimental Section----------3
Figure S1----------6
Figure S2----------6
Figure S3----------7
Figure S4----------7
Figure S5----------8
Figure S6----------8
Figure S7----------9
Figure S8----------9
Figure S9----------10
Figure S10----------10
Table S1----------11
Figure S11----------12
Figure S12----------13
Figure S13----------13
Figure S14----------14
Figure S15----------14
Figure S16----------15
Figure S17----------16
References----------17

Experimental Section

Chemicals and materials: Zinc sulfate heptahydrate ($ZnSO_4 \cdot 7H_2O$, 99.5%), sulfuric acid (H_2SO_4, 98%), and potassium permanganate ($KMnO_4$, 99.5%) were purchased from Sinopharm Chemical Reagent Co., Ltd. Manganese sulfate monohydrate ($MnSO_4 \cdot H_2O$, 99%) and Cyrene ($C_6H_8O_3$, 98.5%) were purchased from Macklin Biochemical Co., Ltd. 1-methyl-2-pyrrolidinone (NMP, 99.5%) was purchased from Aladdin Biochemical Co., Ltd. Zinc foil (thickness: 0.1 mm), copper foil (thickness: 0.03 mm), stainless steel foil (thickness: 0.03 mm), acetylene black (Kappa 100), polyvinylidene fluoride powder (PVDF, 5130), and glass fiber separator (GE-Whatman) were purchased from Canrd Co., Ltd. All chemicals were used as received without additional purification.

Preparation of ZSO/Cyrene mixed electrodes: The ZSO/Cyrene mixed electrodes were prepared by adding a certain amount of Cyrene solvent in 2 M ZSO aqueous solution and stirring for 5 min to obtained a homogeneous solution. The volume ratios of Cyrene to ZSO solution were 2:98 and 5:95, and the obtain electrolytes were denoted ZSO+2% Cyrene and ZSO+5% Cyrene, respectively.

Preparation of MnO_2 cathode: MnO_2 was synthesized using a conventional hydrothermal method. Here, 50 μL H_2SO_4 and 500 mg $MnSO_4 \cdot H_2O$ were added to 60 mL deionized water and stirred continuously for 10 min to obtain a homogeneous solution. Then, 20 mL $KMnO_4$ aqueous solution (with a concentration of 0.1 M) was added slowly to the above solution and stirred continuously for 1 h to form MnO_6 octahedron units. The obtained mixture was then transferred into a 200 mL sealed Teflon-lined autoclave for hydrothermal reaction at 120 °C for 12 h to form crystalline MnO_2. The reacted mixture was then repeatedly centrifuged and washed with deionized water five times, and the resulting product was dried at 60 °C for 24 h to obtain MnO_2 powder. To prepare the MnO_2 cathode, the as-prepared MnO_2 powder was mixed with acetylene black and PVDF powder at a mass ratio of 7:2:1, and NMP was added as the solvent. The obtained slurry was coated on a stainless steel current collector, dried at 80 °C in a vacuum oven for 24 h, and cut into a MnO_2 cathode with a diameter of 12 mm.

Electrochemical measurements: The Zn||Zn symmetric cells, Zn||Cu asymmetric cells, and Zn||MnO_2 full cells were assembled in CR2032 coin cells. Here, 100 μL electrolyte was added into the coin cells, and a glass fiber filter was selected as the separator. The electrochemical performance of the Zn||Zn symmetric cells, Zn||Cu asymmetric cells, and Zn||MnO_2 full cells was collected using a battery test system (LANHE CT3002A). The galvanostatic plating/stripping behaviors of Zn||Zn symmetric cells and Zn||Cu asymmetric cells were measured at different current densities and specific capacities. The galvanostatic discharging/charging measurements of the Zn||MnO_2 full cells and soft-pack cells were conducted at a voltage range of 0.9–1.8 V at different current densities. The linear polarization, LSV, CA, and alternating-current impedance curves were collected using a CHI 760E

electrochemical workstation. In-situ pH tests were performed in an H-type electrolytic cell and two pieces of zinc foil serve as the working electrode and the counter electrode, respectively. The pH value is collected in real time by the zinc counter electrode side through a pH detector. The differential capacitance-potential curves were carried out through alternating current voltammetry (AC) tests in Zn||Cu cells at the scan rate of 5 mV s^{-1} with potential ranging from 0.9 V to 0.1 V (vs. Zn/Zn^{2+}).

Material characterization: The ^{2}H NMR spectral characterizations were performed on a Bruker 400M spectrometer. The FT-IR spectrum (800–3800 cm^{-1}) was measured using a Thermo scientific Nicolet Summit X FTIR spectrometer with attenuated total reflection (ATR) model. Raman spectra were obtained using a Renishaw inVia Raman microscope at an excitation wavelength of 532 nm. The wettability of different aqueous solutions on the zinc foil was tested using the contact angle measurement (Dataphysics OCA15EC). The composition and crystal phase structures of the anodes were detected by XRD (Malvern Panalytical Empyrean) employing Cu Kα radiation from 10° to 80°. The surface and cross-sectional morphologies of the three anodes were observed by field-emission SEM (FE-SEM, Zeiss Gemini 300), and the chemical compositions of the soaked zinc foils were analyzed by X-ray photoelectron spectroscopy (Thermo Fisher Nexsa). The 3D surface topographies of the deposited Zn layer were observed by laser microscopy system (KEYENCE VK-X150). Zeta potential analyzer (Malvern Zetasizer Nano ZS90) was performed to obtain the zeta potentials. The liquid samples were prepared by the thorough ultrasonic treatment of the deposited Zn (2 mA cm^{-2}, 2 mAh cm^{-2}) on the Cu foil in 5 mL electrolyte to form evenly distributed suspensions.

AB initial calculations: The calculations related to adsorption energies between Zn crystal and molecules were performed by VASP package.[S1–S3] In the calculation, the generalized gradient approximation (GGA) with the Perdew-Burke-Ernzerhof (PBE) exchange-correlation functional was adopted.[S4] The energy and force convergence criteria for configurations optimizing were set as 10^{-5} eV and 0.02 eV/Å, respectively. The Zn (002) surface was modeled by a 4×5 supercell that contains four layers of slab and a vacuum region of 15 Å. During the calculations, molecules and the first two layers of Zn (002) were allowed to relax, and the bottom two layers of Zn (002) were fixed at the original position. Brillouin-zone integration was performed using Monkhorst-Pack scheme with a 2×2×1 k-point grid, and the plane wave energy cutoff was set at 400 eV.[S5] The adsorption energy between Zn slab and different molecules is defined as following:

$$E_{ads} = E_{(adsorbate/surface)} - E_{(adsorbate)} - E_{(surface)}$$

where $E_{(adsorbate/surface)}$, $E_{(adsorbate)}$, and $E_{(surface)}$ represent the total energy of the Zn slab and adsorbed species, the adsorbed species, and the Zn slab, respectively.

Quantum chemistry calculations: The density function theory (DFT) method was performed by the Gaussian program.[S6] The structure optimization was performed at PBE0-D3(BJ)/ def2-SVP, and

the single point energy was performed at PBE0-D3(BJ)/ def2-TZVP. The binding energy (E_b) between cations and water/Cyrene molecule is as following:

$$E_b = E_{complex} - E_c - E_m$$

where $E_{complex}$, E_c, and E_m represent the total energy of the complex, the total energy of cation, and the energy of water or Cyrene, respectively. The Electrostatic potential (ESP) was analyzed by Multiwfn package and VMD package.[S7,S8]

Molecular dynamics (MD) simulations: MD simulations were performed using the GROMACS package.[S9] The force field parameters were obtained from the GAFF force fields generated by Sobtop.[S10] The TIP3P water model was employed for water molecules. The initial size of the box was set at 110×110×110 nm^3, and the box contained 2744 H_2O, 100 $ZnSO_4$, and 16 Cyrene molecules. PME methods was used to calculated the electrostatic interactions and a cutoff of 1.0 nm was set in the calculation of electrostatic interactions and non-electrostatic interactions in real space. The details of MD simulations are as follows: The system was annealed from 0 to 298 K over a period of 0.5 ns, following by running for another 2.0 ns to reach equilibrium. The temperature and pressure coupling were adopted V-rescale and Berendsen method, respectively. Finally, a 10-ns production simulation was run for post-processing analysis. The pressure coupling method in production simulation period was changed to Parrinello-Rahman and the pressure was maintained at 1 atm.

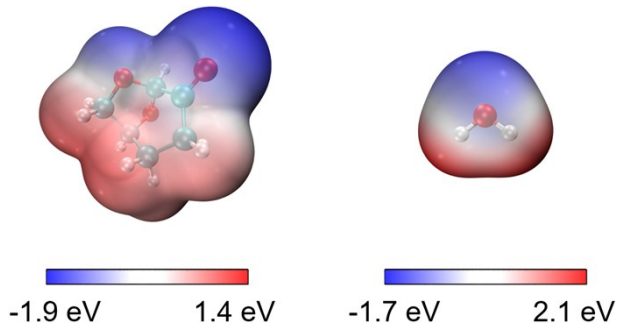

Figure S1. Electrostatic potential mapping of the Cyrene (left) and H_2O (right) molecules.

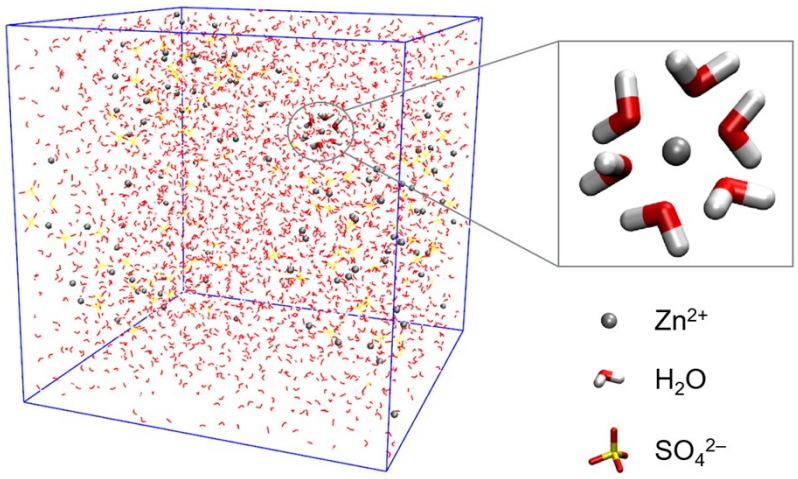

Figure S2. 3D snapshot of pristine ZSO aqueous solution obtained from MD simulations.

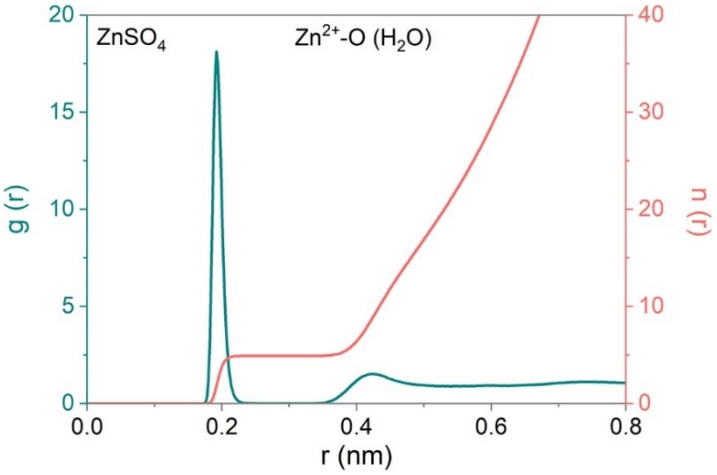

Figure S3. The RDFs results for Zn–O collected from MD simulations in pristine ZSO aqueous solution.

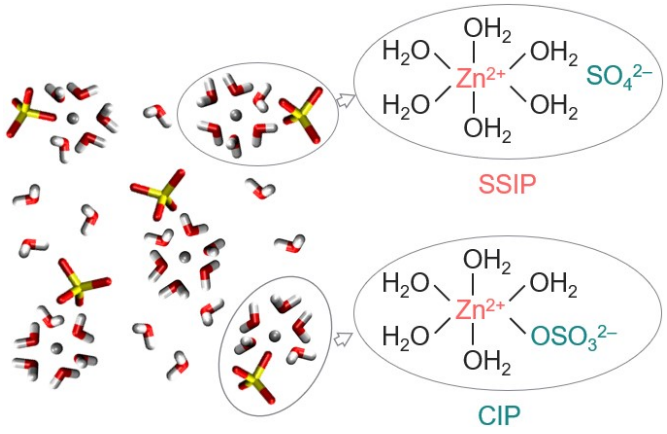

Figure S4. Schematic illustration for the two solvation structures in ZSO aqueous solutions.

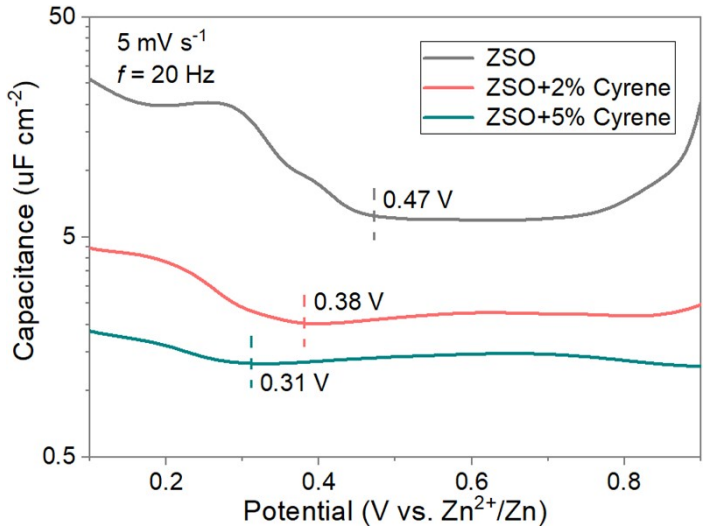

Figure S5. The differential capacitance curves conducted in ZSO, ZSO+2% Cyrene, and ZSO+5% Cyrene electrolytes.

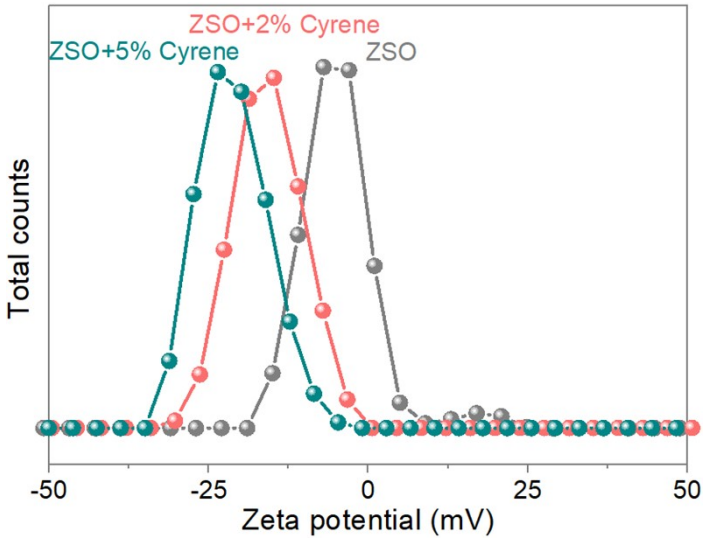

Figure S6. Zeta potential of the Zn particles dispersed in ZSO, ZSO+2% Cyrene, and ZSO+5% Cyrene electrolytes.

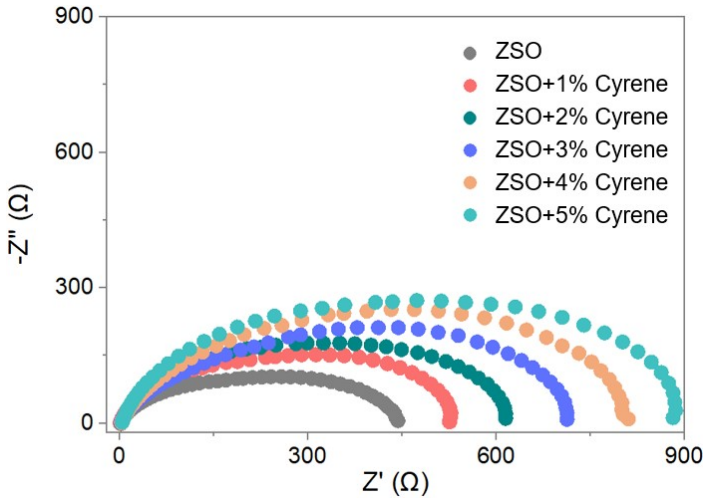

Figure S7. Nyquist plots of Zn||Zn symmetric cells tested at room temperature using ZSO electrolytes containing with different content of Cyrene solvent.

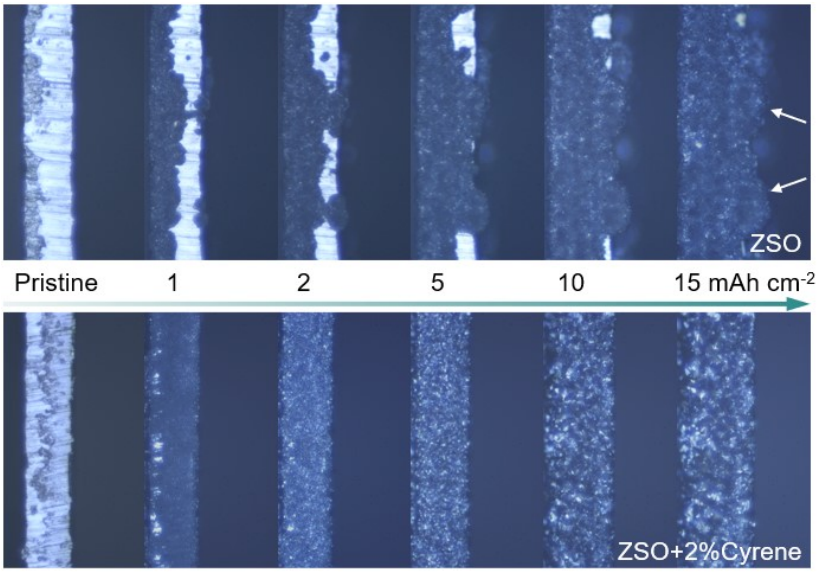

Figure S8. In situ optical microscopic observations of the deposited Zn anode surface in ZSO and ZSO+2% Cyrene electrolytes at the current density of 10 mA cm^{-2}.

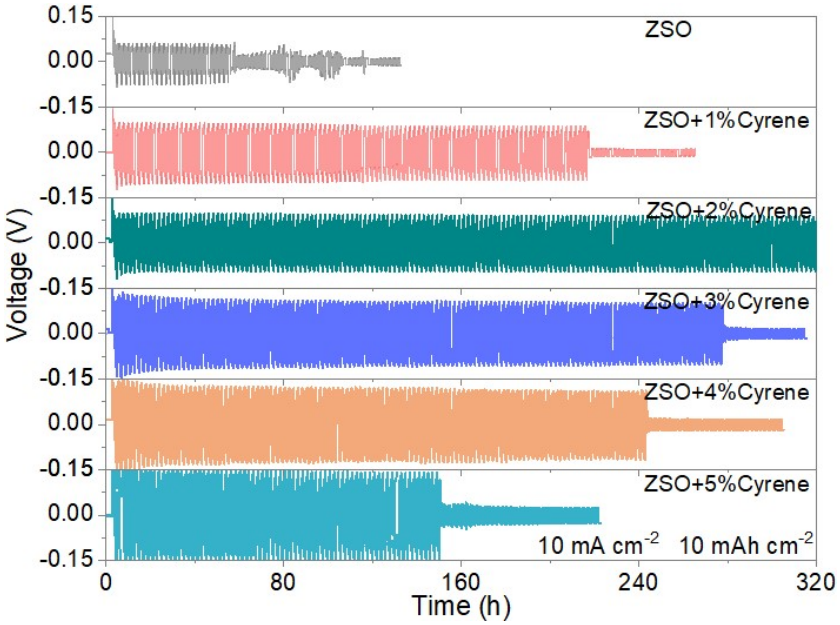

Figure S9. Galvanostatic charge/discharge profiles of Zn||Zn symmetric cells at 10 mA cm^{-2} and 10 mAh cm^{-2}.

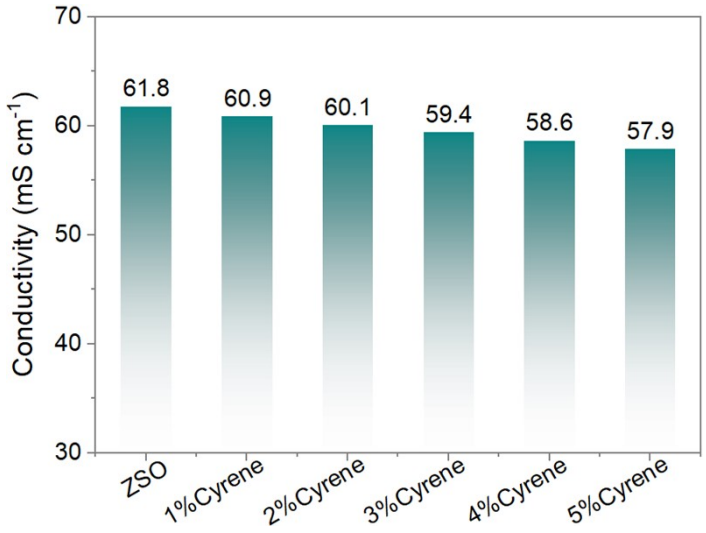

Figure S10. Ionic conductivity of ZSO systems containing with different content of Cyrene.

Table S1. Comparison of cycling life, addition amount, and cost of reported liquid organic electrolyte additives. Note that, the prices are obtained from the official website of Aladdin.

Liquids	Addition amount	Cycling time	Cost [¥]	Ref.
Cyrene	2 vol%	4250 h @ 1 mA cm^{-2} & 1 mAh cm^{-2} 2000 h @ 5 mA cm^{-2} & 5 mAh cm^{-2}	1600/500 mL	This work
Dimethyl sulfoxide	18.9 vol%	1000 h @ 0.5 mA cm^{-2} & 0.5 mAh cm^{-2}	124/500 mL	27
Acetonitrile	25 vol%	1300 h @ 1 mA cm^{-2} & 1 mAh cm^{-2}	63/500 mL	S11
Methanol	50 vol%	--	60/500 mL	26
Glycerol	50 vol%	1500 h @ 1 mA cm^{-2} & 1 mAh cm^{-2}	58/500 mL	S12
Ethylene glycol	40 vol%	80 h @ 2 mA cm^{-2} & 1 mAh cm^{-2}	66/500 mL	S13
Triethyl phosphate	70 vol%	2000 h @ 0.5 mA cm^{-2} & 5 mAh cm^{-2}	93/500 mL	S14
N-methyl-2-pyrrolidone	5 vol%	540 h @ 1 mA cm^{-2} & 1 mAh cm^{-2}	73/500 mL	51
Acetonitrile	10 vol%	600 h @ 2 mA cm^{-2} & 2 mAh cm^{-2}	63/500 mL	S15
N, N-dimethyl acetamide	10 vol%	1000 h @ 3 mA cm^{-2} & 3 mAh cm^{-2}	70/500 mL	S16
1,2-dimethoxyethane	40 vol%	1100 h @ 5 mA cm^{-2} & 2.5 mAh cm^{-2}	1508/8 mL	S17
Ethanol	95 vol%	650 h @ 0.5 mA cm^{-2} & 0.5 mAh cm^{-2}	53/500 mL	S18
Diethyl carbonate	85 vol%	700 h @ 5 mA cm^{-2} & 5 mAh cm^{-2}	74/500 mL	18

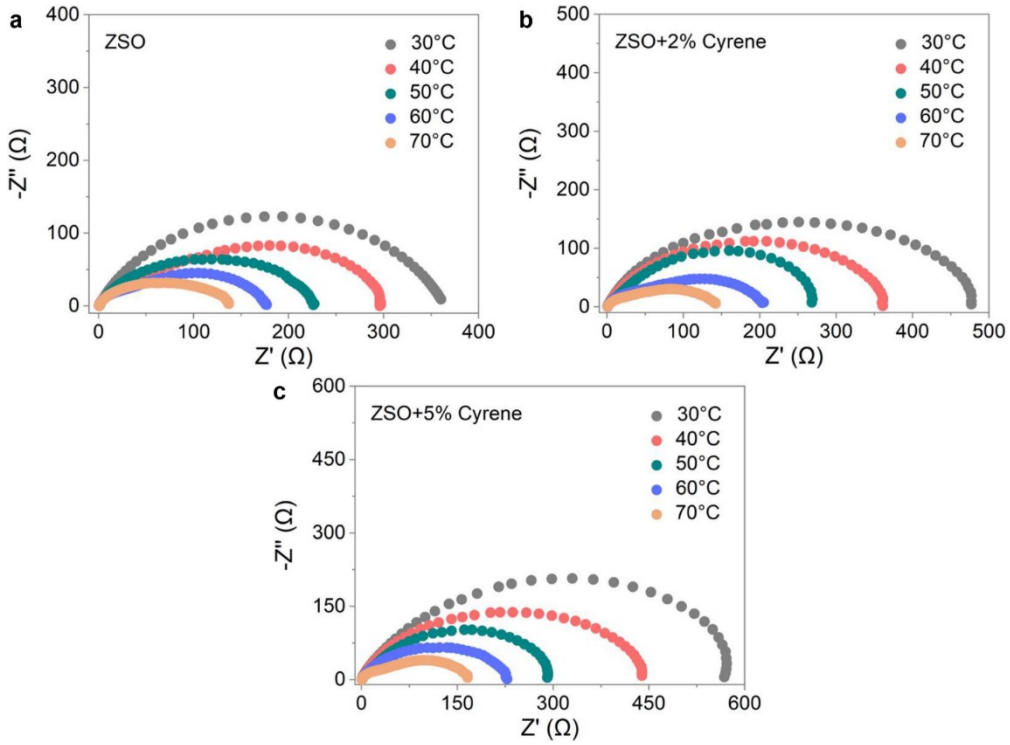

Figure S11. Nyquist plots of Zn||Zn symmetric cells tested at different temperatures using (a) ZSO, (b) ZSO+2% Cyrene, and (c) ZSO+5% Cyrene electrolytes.

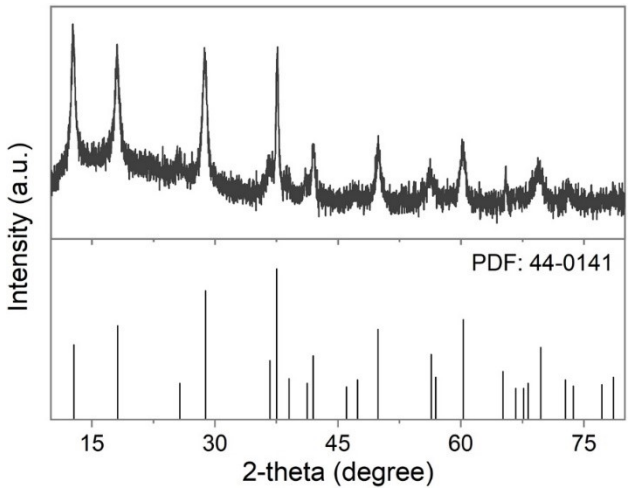

Figure S12. XRD pattern of the synthesized MnO_2 sample and the standard diffraction pattern of α-MnO_2 (JCPDS 44-0141).

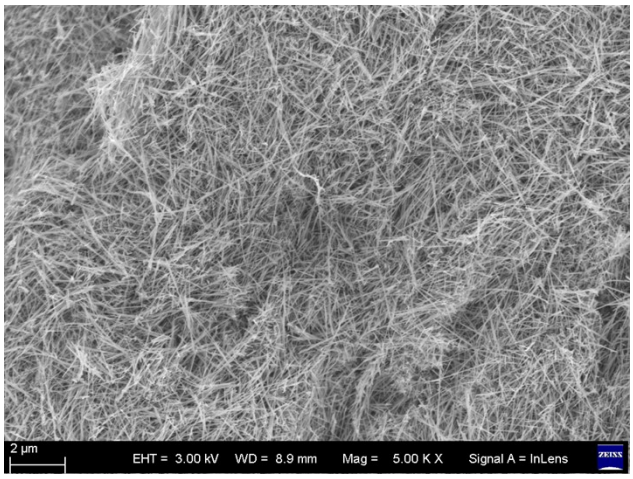

Figure S13. SEM image of the synthesized MnO_2 sample.

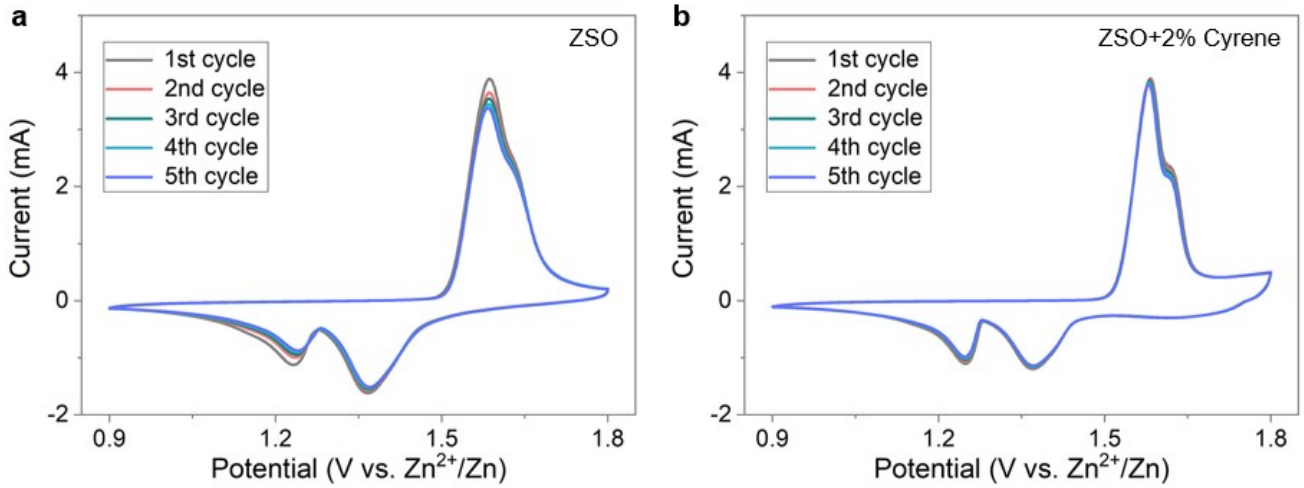

Figure S14. Initial five CV curves of the MnO_2-based full cells using (a) ZSO and (b) ZSO+2% Cyrene electrolytes at a sweep rate of 0.5 mV s^{-1}.

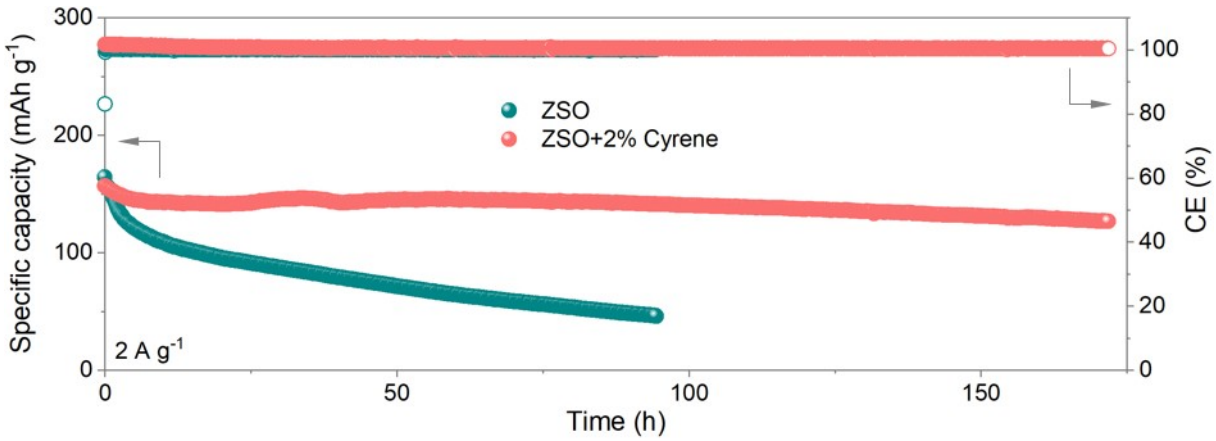

Figure S15. Specific capacity versus cycling time plots of the MnO_2-based full cells using different electrolytes.

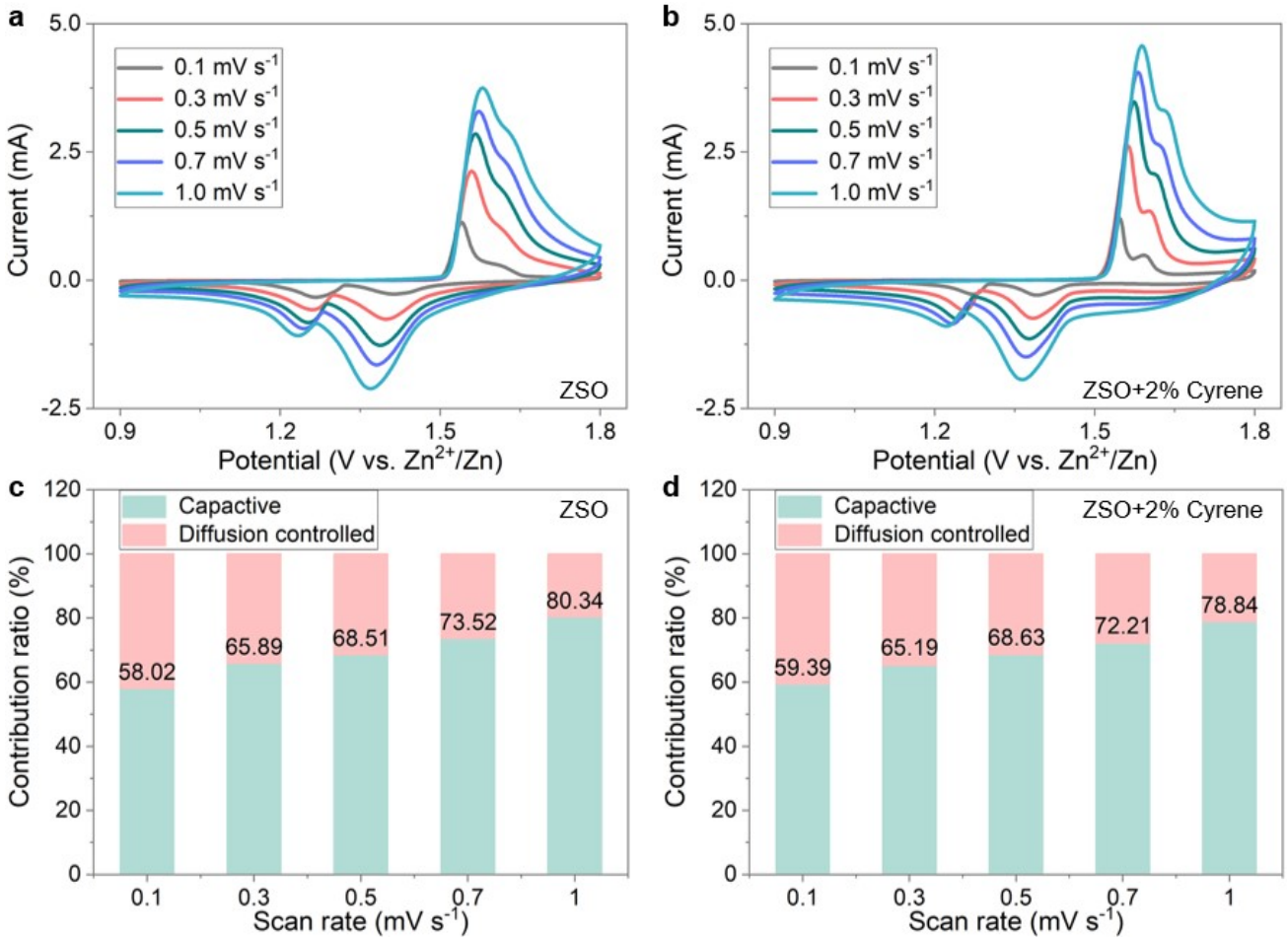

Figure S16. CV profiles of the full cells using (a) ZSO and (b) ZSO+2% Cyrene electrolytes at different scan rates. Bar chart showing the percentage of calculated capacitive contribution of the full cells using (c) ZSO and (d) ZSO+2% Cyrene electrolytes at different scan rates.

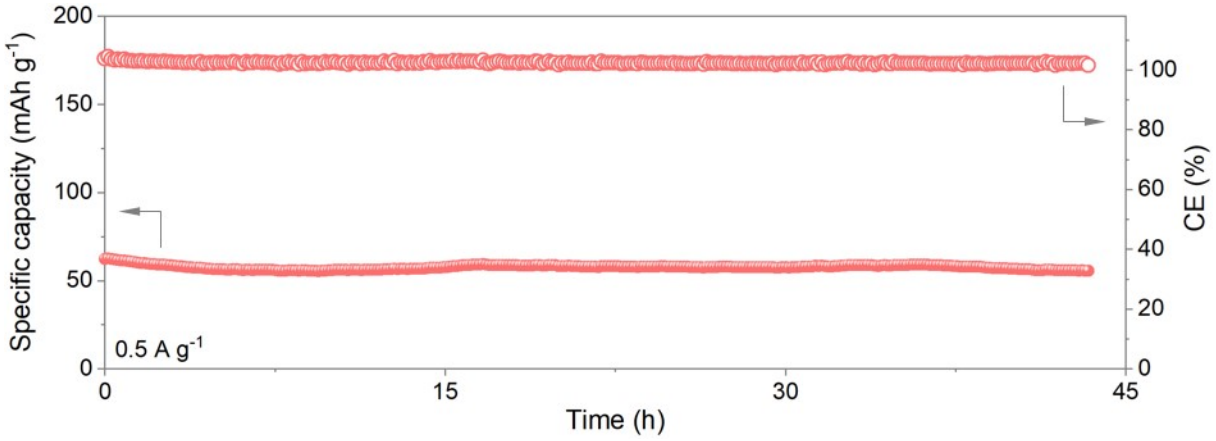

Figure S17. Specific capacity versus cycling time plots of the MnO_2-based pouch cell using ZSO+2% Cyrene electrolyte.

References

S1. G. Kresse and J. Furthmüller, *Phy. Rev. B*, 1996, **54**, 11169.

S2. G. Kresse and J. Furthmüller, *Comp. Mater. Sci.*, 1996, **6**, 15–50.

S3. G. Kresse and D. Joubert, *Phys. Rev. B*, 1999, **59**, 1758.

S4. J. P. Perdew, K. Burke and M. Ernzerhof, *Phys. Rev. Lett.*, 1996, **77**, 3865.

S5. H. J. Monkhorst and J. D. Pack, *Phys. Rev. B*, 1976, **13**, 5188.

S6. M. Frisch, G. Trucks, H. Schlegel, G. Scuseria, M. Robb, J. Cheeseman, G. Scalmani, V. Barone, B. Mennucci and G. Petersson, In Gaussian 09, Gaussian Inc Wallingford: 2009.

S7. W. Humphrey, A. Dalke and K. Schulten, *J. Mol. Graph.*, 1996, **14**, 33–38.

S8. T. Lu and F. Chen, *J. Comput. Chem.*, 2012, **33**, 580–592.

S9. B. Hess, C. Kutzner, D. Van Der Spoel and E. Lindahl, *J. Chem. Theory Comput.*, 2008, **4**, 435–447.

S10. T. Lu, Sobtop, Version 1.0 (dev3. 1).

S11. J. Shi, K. Xia, L. Liu, C. Liu, Q. Zhang, L. Li, X. Zhou, J. Liang and Z. Tao, *Electrochim. Acta*, 2020, **358**, 136937.

S12. Y. Zhang, M. Zhu, K. Wu, F. Yu, G. Wang, G. Xu, M. Wu, H.K. Liu, S. X. Dou and C. Wu, *J. Mater. Chem. A*, 2021, **9**, 4253–4261.

S13. N. Chang, T. Li, R. Li, S. Wang, Y. Yin, H. Zhang and X. Li, *Energy Environ. Sci.*, 2020, **13**, 3527–3535.

S14. A. Naveed, H. Yang, J. Yang, Y. Nuli and J. Wang, *Angew. Chem. Int. Ed.*, 2019, **58**, 2760–2764.

S15. Z. Hou, H. Tan, Y. Gao, M. Li, Z. Lu and B. Zhang, *J. Mater. Chem. A*, 2020, 8, 19367–19374.

S16. W. Deng, Z. Xu and X. Wang, *Energy Storage Mater.*, 2022, **52**, 52–60.

S17. G. Ma, L. Miao, Y. Dong, W. Yuan, X. Nie, S. Di, Y. Wang, L. Wang and N. Zhang, *Energy Storage Mater.*, 2022, **47**, 203–210.

S18. Y. Sun, Z. Xu, X. Xu, Y. Nie, J. Tu, A. Zhou, J. Zhang, L. Qiu, F. Chen, J. Xie, T. Zhu and X. Zhao, *Energy Storage Mater.*, 2022, **48**, 192–204.